ANP AUTHORIZATION REQUIRED
ORNL-1924
Reactors-Aircraft Nuclear Propulsion Systems

AEC RESEARCH AND DEVELOPMENT REPORT

A THEORETICAL STUDY OF Xe^{135} POISONING KINETICS IN FLUID-FUELED, GAS-SPARGED NUCLEAR REACTORS

M. T. Robinson

OAK RIDGE NATIONAL LABORATORY
OPERATED BY
UNION CARBIDE NUCLEAR COMPANY
A Division of Union Carbide and Carbon Corporation
UCC
POST OFFICE BOX P · OAK RIDGE, TENNESSEE

[redacted]

ANP Authorization Required

ORNL-1924

This document consists of 29 pages.

Copy 137 of 220 copies. Series A.

Contract No. W-7405-eng-26

SOLID STATE DIVISION

A THEORETICAL STUDY OF Xe^{135} POISONING KINETICS IN FLUID-FUELED, GAS-SPARGED NUCLEAR REACTORS

M. T. Robinson

DATE ISSUED

FEB 6 1956

OAK RIDGE NATIONAL LABORATORY
Operated by
UNION CARBIDE NUCLEAR COMPANY
A Division of Union Carbide and Carbon Corporation
Post Office Box P
Oak Ridge, Tennessee

[redacted]

[redacted]

ANP AUTHORIZATION REQUIRED
ORNL-1924
Reactors-Aircraft Nuclear Propulsion Systems
TID-4679 (17th ed.)

INTERNAL DISTRIBUTION

1. R. G. Affel
2. C. R. Baldock
3. C. J. Barton
4. C. D. Baumann
5. R. G. Berggren
6. J. O. Betterton, Jr.
7. D. S. Billington
8. D. Binder
9. F. F. Blankenship
10. T. H. Blewitt
11. E. P. Blizard
12. C. D. Bopp
13. C. J. Borkowski
14. G. E. Boyd
15. M. A. Bredig
16. H. Brooks (consultant)
17. W. E. Browning
18. F. R. Bruce
19. W. E. Brundage
20. A. D. Callihan
21. D. W. Cardwell
22. J. V. Cathcart
23. C. E. Center
24. R. A. Charpie
25. J. W. Cleland
26. G. H. Clewett
27. C. E. Clifford
28. A. F. Cohen
29. J. H. Coobs
30. W. B. Cottrell
31. D. D. Cowen
32. J. H. Crawford, Jr.
33. S. Cromer
34. R. S. Crouse
35. F. L. Culler
36. J. E. Cunningham
37. J. B. Dee
38. J. H. DeVan
39. R. R. Dickison
40. S. E. Dismukes
41. D. A. Douglas
42. E. R. Dytlewski
43. L. B. Emlet (K-25)
44. M. J. Feldman
45. D. E. Ferguson
46. A. P. Fraas
47. J. H. Frye, Jr.
48. W. T. Furgerson
49. J. L. Gabbard
50. H. C. Gray
51. R. J. Gray
52. W. R. Grimes
53. W. O. Harms (consultant)
54. C. S. Harrill
55. E. E. Hoffman
56. A. Hollaender
57. D. K. Holmes
58. A. S. Householder
59. J. T. Howe
60. L. K. Jetter
61. R. J. Jones
62. W. H. Jordan
63. G. W. Keilholtz
64. C. P. Keim
65. M. T. Kelley
66. R. H. Kernohan
67. F. Kertesz
68. E. M. King
69. H. V. Klaus
70. G. E. Klein
71. J. A. Lane
72. T. A. Lincoln
73. S. C. Lind
74. R. S. Livingston
75. R. N. Lyon
76. H. G. MacPherson (consultant)
77. F. C. Maienschein
78. W. D. Manly
79. E. R. Mann
80. L. A. Mann
81. W. B. McDonald
82. F. W. McQuilkin
83. R. V. Meghreblian
84. A. J. Miller
85. E. C. Miller
86. J. G. Morgan
87. K. Z. Morgan
88. E. J. Murphy

[redacted]

89. J. P. Murray (Y-12)
90. G. J. Nessle
91. R. B. Oliver
92. P. Patriarca
93. W. W. Parkinson
94. R. W. Peelle
95. A. M. Perry
96. W. G. Piper
97. H. F. Poppendiek
98. P. M. Reyling
99. M. T. Robinson
100. H. W. Savage
101. A. W. Savolainen
102. R. D. Schultheiss
103. H. C. Schweinler
104. F. Seitz (consultant)
105. E. D. Shipley
106. A. Simon
107. O. Sisman
108. M. J. Skinner
109. G. P. Smith
110. A. H. Snell
111. R. L. Sproull (consultant)
112. E. E. Stansbury
113. D. K. Stevens
114. W. J. Sturm
115. C. D. Susano
116. J. A. Swartout
117. E. H. Taylor
118. D. B. Trauger
119. J. B. Trice
120. E. R. Van Artsdalen
121. F. C. VonderLage
122. J. M. Warde
123. C. M. Watson
124. E. C. Webster
125. M. S. Wechsler
126. R. A. Weeks
127. A. M. Weinberg
128. J. C. White
129. G. D. Whitman
130. E. P. Wigner (consultant)
131. G. C. Williams
132. W. R. Willis
133. J. C. Wilson
134. C. E. Winters
135. M. C. Wittels
136. Biology Library
137-138. Central Research Library
139. Health Physics Library
140-142. Laboratory Records Department
143. Laboratory Records, ORNL R.C.
144. ORNL – Y-12 Technical Library, Document Reference Section
145. Reactor Experimental Engineering Library

EXTERNAL DISTRIBUTION

146. AF Plant Representative, Baltimore
147. AF Plant Representative, Burbank
148. AF Plant Representative, Marietta
149. AF Plant Representative, Santa Monica
150. AF Plant Representative, Seattle
151. AF Plant Representative, Wood-Ridge
152. Air Research and Development Command (RDGN)
153. Air Research and Development Command (RDZPA)
154. Air Technical Intelligence Center
155. Air University Library
156. Aircraft Laboratory Design Branch (WADC)
157-159. ANP Project Office, Fort Worth
160. Argonne National Laboratory
161. Armed Forces Special Weapons Project, Sandia
162. Assistant Secretary of the Air Force, R&D
163-168. Atomic Energy Commission, Washington
169. Bureau of Aeronautics
170. Bureau of Aeronautics General Representative
171. Chicago Operations Office

[redacted]

172. Chicago Patent Group
173-174. Chief of Naval Research
175. Convair-General Dynamics Corporation
176. Director of Laboratories (WCL)
177. Director of Requirements (AFDRQ)
178. Director of Research and Development (AFDRD-ANP)
179-181. Directorate of Systems Management (RDZ-ISN)
182-184. Directorate of Systems Management (RDZ-ISS)
185. Equipment Laboratory (WADC)
186-189. General Electric Company (ANPD)
190. Hartford Area Office
191. Headquarters, Air Force Special Weapons Center
192. Lockland Area Office
193. Los Alamos Scientific Laboratory
194. Materials Laboratory, Systems Office (WADC)
195. National Advisory Committee for Aeronautics, Cleveland
196. National Advisory Committee for Aeronautics, Washington
197. North American Aviation, Inc. (Aerophysics Division)
198. Nuclear Development Corporation
199. Patent Branch, Washington
200-202. Power Plant Laboratory (WADC)
203-206. Pratt and Whitney Aircraft Division (Fox Project)
207. Sandia Corporation
208. School of Aviation Medicine
209. USAF Project Rand
210. University of California Radiation Laboratory, Livermore
211-213. Wright Air Development Center (COSI-3)
214-219. Technical Information Service, Oak Ridge
220. Division of Research and Development, AEC, ORO

[redacted]

[redacted]

CONTENTS

1. Introduction 1
2. Derivation of the Differential Equations 1
3. Relations Between the Various Phase-Transfer Rate Constants 4
4. Solution of the Differential Equations 6
5. Steady-State Operation of a Reactor 9
6. Kinetics of Xe^{135} Poisoning in the ARE 12
7. Kinetics of Xe^{135} Poisoning in the ART 15
8. Kinetics of Xe^{135} Poisoning During Shutdowns 18
9. Nomograms for Xenon-Poisoning Calculations 18

[redacted]

[redacted]

A THEORETICAL STUDY OF Xe^{135} POISONING KINETICS IN FLUID-FUELED, GAS-SPARGED NUCLEAR REACTORS

M. T. Robinson

1. INTRODUCTION

One of the substantial advantages claimed for liquid fuels in very-high-power nuclear reactors is the easy removal of Xe^{135} from the fuel, with the consequent gains in neutron economy.[1] This claim is at least partly supported by operating experience with the ARE.[2] This report is concerned with a theoretical study of the kinetics of Xe^{135} poisoning in a reactor in which this volatile poison is continuously removed by a stream of sparging gas. The theory is applied to the experience with the ARE and is used to make predictions for the ART. Some comments on full-scale aircraft power plants are also included.

The system is assumed to consist of two phases: the liquid fuel and the sparging gas. The theory is concerned only with *volume-averaged* concentrations and neutron fluxes. Turbulent motion of the two fluids is held to assure thorough mixing within each phase. The appropriate differential equations which describe the behavior of the poisoning in such a system are derived and solved. Steady-state behavior during high-power operation of the reactor is discussed. Detailed kinetics of the poisoning during the approach to steady state are studied through a series of calculations performed on the Oracle. A brief discussion of shutdown behavior follows. A final section presents a rapid approximate method for calculating Xe^{135} poisoning in gas-sparged fluid-fueled reactors.

2. DERIVATION OF THE DIFFERENTIAL EQUATIONS

The volume-averaged concentration of Xe^{135} in the fuel of a fluid-fueled nuclear reactor changes because of a number of different processes, as shown schematically in Fig. 1. These

[1] W. R. Grimes *et al.*, *The Reactor Handbook*, vol 2 (September 1953), p 973.

[2] M. T. Robinson, W. A. Brooksbank, and D. E. Guss, *ANP Quar. Prog. Rep. Dec. 10, 1954*, ORNL-1816, p 124–125.

[redacted]

SSD-A-1167
ORNL-LR-DWG 6430A

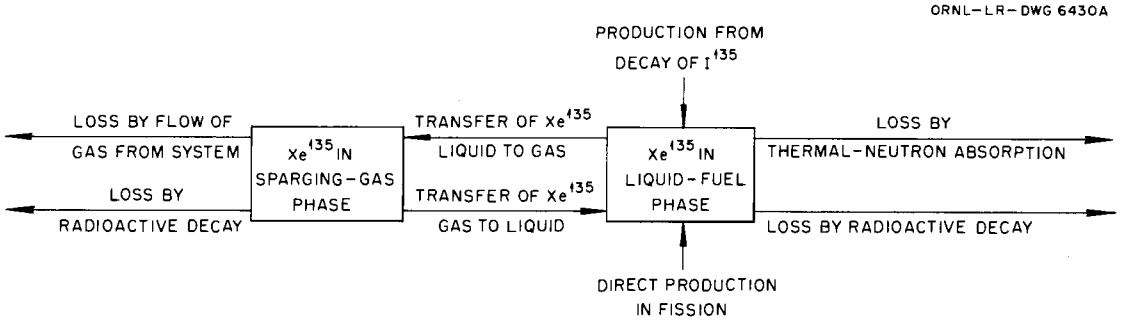

Fig. 1. Processes Governing Xe^{135} Poisoning in Fluid-Fueled Reactors.

[redacted]

processes are as follows (see Table 1 for definitions of all symbols used):

1. direct production from fission,

$$\text{Rate 1} = \gamma_{Xe}\Sigma_f\phi \ ; \tag{2.1}$$

2. production from decay of I^{135},

$$\text{Rate 2} = \gamma_I\Sigma_f\phi(1 - e^{-\alpha_3 t}) \ ; \tag{2.2}$$

3. transfer from the gas phase to the liquid phase,

$$\text{Rate 3} = \frac{\lambda_r c_G V_G}{V_L} \ ; \tag{2.3}$$

TABLE 1. DEFINITION OF SYMBOLS

English Letters	Definition	Greek Letters	Definition
A	Area of liquid-gas boundary surface	α_0	$100\gamma_{Xe}\sigma_f/\sigma_u$
a_G	Activity of Xe^{135} in the gas phase	α_1	$100\gamma_I\sigma_f/\sigma_u$
a_L	Activity of Xe^{135} in the liquid phase	α_2	$\lambda_r/\beta\lambda_f = RTS$; see Eq. 3.4
c_G	Concentration of Xe^{135} in gas phase	α_3	Radioactive decay constant of I^{135}
c_L	Concentration of Xe^{135} in liquid phase	α_4	Radioactive decay constant of Xe^{135}
$\mathcal{I}_0$	Concentration of I^{135} at $t = 0$; see Eq. 4.18	β	V_L/V_G
k'	Mass-transfer film coefficient	γ_I	Fission yield of I^{135}
k_1	$\alpha_4 + \lambda_f + \lambda_L$	γ_{Xe}	Fission yield of Xe^{135}
k_2	$\alpha_4 + \alpha_2\beta\lambda_f + \lambda_g$	λ_f	Rate constant for transfer of xenon from liquid to gas
p_G	Partial pressure of Xe^{135} in gas phase	λ_g	v_G/V_G
Q'	Rate of mass transfer	λ_L	$\sigma_{Xe}\phi$
R	Universal gas constant	λ_r	Rate constant for transfer of xenon from gas to liquid
S	Solubility coefficient of xenon in fuel	σ_f	Microscopic fission cross section of U^{235}
T	Absolute temperature	Σ_f	Macroscopic fission cross section of fuel
t	Time	σ_u	Microscopic neutron absorption cross section of U^{235}
v_G	Volumetric flow rate of sparging gas	Σ_u	Macroscopic neutron absorption cross section of fuel
V_G	Volume of gas phase	σ_{Xe}	Microscopic neutron absorption cross section of Xe^{135}
V_L	Volume of liquid phase	ϕ	Volume-averaged thermal-neutron flux
x	Xe^{135} poisoning in fuel		
y	"Equivalent poisoning" in gas phase; see Eq. 2.14		

4. loss by radioactive decay,

$$\text{Rate 4} = -\alpha_4 c_L \ ; \tag{2.4}$$

5. loss by absorption of thermal neutrons,

$$\text{Rate 5} = -\sigma_{Xe}\phi c_L \ ; \tag{2.5}$$

6. loss by transfer to the gas phase,

$$\text{Rate 6} = -\lambda_f c_L \ . \tag{2.6}$$

The over-all time dependence of the Xe^{135} concentration in the liquid phase is given by the sum of these six rates:

$$\dot{c}_L = \gamma_{Xe}\Sigma_f\phi + \gamma_I\Sigma_f\phi(1 - e^{-\alpha_3 t}) + \frac{V_G}{V_L}\lambda_r c_G - (\alpha_4 + \sigma_{Xe}\phi + \lambda_f)c_L \ . \tag{2.7}$$

The processes which change the volume-averaged Xe^{135} concentration in the gas phase are as follows:

7. transfer from the liquid phase,

$$\text{Rate 7} = \frac{\lambda_f c_L V_L}{V_G} \ ; \tag{2.8}$$

8. loss by radioactive decay,

$$\text{Rate 8} = -\alpha_4 c_G \ ; \tag{2.9}$$

9. loss by transfer to the liquid phase,

$$\text{Rate 9} = -\lambda_r c_G \ ; \tag{2.10}$$

10. loss by flow of gas out of the reactor,

$$\text{Rate 10} = -\frac{v_G c_G}{V_G} \ . \tag{2.11}$$

Several ways in which changes might occur in the concentration of Xe^{135} in the gas phase have been specifically neglected; these are:

11. loss by absorption of thermal neutrons;
12. production from decay of I^{135} or from fission. This implies the neglect of transfer processes (like 3, 7, 9, and 10) involving I^{135} or U^{235}.

The over-all time dependence of the Xe^{135} concentration in the gas phase is given by the sum of processes 7 through 10 to be

$$\dot{c}_G = \frac{V_L}{V_G}\lambda_f c_L - \left(\alpha_4 + \lambda_r + \frac{v_G}{V_G}\right) c_G \ . \tag{2.12}$$

In this discussion of the behavior of a nuclear reactor, the behavior of the Xe^{135} poisoning

is of primary interest and is defined as

$$x = \frac{100\sigma_{Xe}c_L}{\Sigma_u} \quad . \tag{2.13}$$

The related quantity y is defined as

$$y = \frac{100\sigma_{Xe}c_G}{\Sigma_u} \quad . \tag{2.14}$$

The virtue of this latter quantity stems from the identity

$$\frac{x}{y} = \frac{c_L}{c_G} \quad , \tag{2.15}$$

which will be required in deriving a relationship between λ_f and λ_r. By the use of Eqs. 2.7, 2.12, 2.13, and 2.14 and some abbreviations from Table 1, the differential equations for the poisoning are written as

$$\dot{x} = \alpha_0\lambda_L + \alpha_1\lambda_L(1 - e^{-\alpha_3 t}) + \alpha_2\lambda_f y - (\alpha_4 + \lambda_f + \lambda_L)x \; ; \tag{2.16}$$

$$\dot{y} = \beta\lambda_f x - (\alpha_4 + \alpha_2\beta\lambda_f + \lambda_g)y \quad . \tag{2.17}$$

The above equations apply during the nuclear power operation of a reactor. However, the behavior of the poisoning during a shutdown must also be discussed. In this case it is necessary to set $\lambda_L = 0$ and to replace the first two terms of Eq. 2.16 by the source term

$$\alpha_3\mathfrak{d}_0 e^{-\alpha_3 t} \quad . \tag{2.18}$$

The boundary conditions needed in solving Eqs. 2.16 and 2.17 are discussed in Sec. 4.

3. RELATIONS BETWEEN THE VARIOUS PHASE-TRANSFER RATE CONSTANTS

The problem of studying the kinetics of Xe^{135} poisoning can be simplified by eliminating one of the phase-transfer rate constants, defined in Eqs. 2.6 and 2.10. The total rate of transfer of xenon from the liquid phase to the gas phase is $\lambda_f V_L c_L$. The total rate of transfer in the reverse direction is $\lambda_r V_G c_G$. Now, while it probably cannot be realized in practice, there exists some pair of values (c_G^*, c_L^*) corresponding to true thermodynamic equilibrium between the two phases. The "law of mass action"[3] requires that under these conditions the amount of material entering a phase be the same as the amount leaving, that is, that

$$\lambda_f V_L c_L^* = \lambda_r V_G c_G^*$$

or

$$\lambda_r = \lambda_f \frac{V_L}{V_G} \frac{c_L^*}{c_G^*} \quad . \tag{3.1}$$

[3] C. M. Guldberg and P. Waage, *Etudes sur les affinities chimiques*, 1867.

The solubility coefficient of a gas in a liquid is the equilibrium concentration of solute in the liquid phase when the partial pressure of the substance in the gas phase is 1 atm. That is,

$$c_L^* = p_G^* S = c_G^* RTS \ , \tag{3.2}$$

where the ideal gas law has been used in the form

$$p_G = c_G RT$$

to relate the Xe^{135} pressure to its concentration in the gas phase. A combination of Eqs. 2.1 and 3.2 gives the desired result:

$$\lambda_r = \lambda_f RTS \frac{V_L}{V_G} \ , \tag{3.3}$$

whence

$$\alpha_2 = RTS \ . \tag{3.4}$$

Thus equilibrium solubility data may be used to eliminate the rate constant λ_r.

Also, a relation may be derived between the "true" rate constants, λ_f and λ_r, and the "apparent" rate constant,[4] λ_p. The latter is defined by

$$\text{Net } Xe^{135} \text{ transfer rate} = -\lambda_p c_L \ . \tag{3.5}$$

Equating this to the sum of rates defined in Eqs. 2.3 and 2.6, it is found that

$$\lambda_p = \lambda_f - \lambda_r \frac{V_G}{V_L} \frac{c_G}{c_L} \ , \tag{3.6}$$

or, introducing Eq. 3.3,

$$\lambda_p = \lambda_f \left(1 - RTS \frac{c_G}{c_L} \right) \ . \tag{3.7}$$

If Eqs. 3.4 and 2.15 are introduced, then

$$\lambda_p = \lambda_f \left(1 - \frac{\alpha_2 y}{x} \right) \ . \tag{3.8}$$

Thus experimentally derived values of λ_p may be compared with values calculated from the solutions to Eqs. 2.16 and 2.17.

The connection of the rate constant λ_f to the usual mass-transfer film coefficient may be shown by noting that the total net current of matter across the boundary between the liquid and gas phases is

$$Q' = -\lambda_f V_L c_L + \lambda_r V_G c_G = -\lambda_f V_L (c_L - RTS\, c_G) \ . \tag{3.9}$$

According to the usual mass-transfer analysis,[5] the total current may be written as

$$Q' = -k' A (a_L - a_G) \ . \tag{3.10}$$

---

[4] J. L. Meem, *The Xenon Problem in the ART*, ORNL CF-54-5-1 (May 3, 1954).

[5] G. G. Brown *et al.*, *Unit Operations*, p 510 ff, Wiley, New York, 1950.

Both phases are assumed to be ideal. The xenon activity in the liquid may be replaced by the concentration. Therefore the standard state in the gas phase must be considered as that pressure of xenon in equilibrium with unit concentration in the liquid. Thus

$$a_G = p_G S = RTS\, c_G \ .$$

Then Eq. 3.10 becomes

$$Q' = -k'A(c_L - RTS\, c_G) \ . \tag{3.11}$$

Comparison of Eqs. 3.9 and 3.11 yields

$$\lambda_f = \frac{k'A}{V_L} \ . \tag{3.12}$$

In principle, the film coefficient k' can be computed from the geometry of the system and the physical properties and flow rate of the liquid fuel through a relation of the type

$$\frac{k's}{D_L} = f(Sc, Re) \ , \tag{3.13}$$

where s is a characteristic dimension; D_L is the diffusion coefficient of Xe^{135} in the liquid; Re is the Reynolds number of the liquid; and Sc, the Schmidt number, is given by

$$Sc = \frac{\nu_L}{D_L} \ ,$$

in which ν_L is the kinematic viscosity of the liquid. It does not appear practical to calculate λ_f in this way, because of the complicated geometry and flow regime obtaining in the ARE and ART.

4. SOLUTION OF THE DIFFERENTIAL EQUATIONS

The time dependence of the poisoning of a nuclear reactor due to Xe^{135} may be expressed by the differential equations

$$\dot{x} = f_n(t) + \alpha_2\lambda_f y - k_1 x \tag{4.1}$$

and

$$\dot{y} = \beta\lambda_f x - k_2 y \ . \tag{4.2}$$

The source term is

$$f_1(t) = \alpha_0\lambda_L + \alpha_1\lambda_L(1 - e^{-\alpha_3 t}) \tag{4.3}$$

when the reactor is in operation and

$$f_2(t) = \alpha_3 \mathfrak{I}_0 e^{-\alpha_3 t} \tag{4.4}$$

otherwise. The quantity $\mathfrak{I}_0$ is related to the amount of I^{135} present at $t = 0$.

By solving Eq. 4.2 for x, differentiating with respect to t, and combining the results with

Eq. 4.1, the differential equation

$$\ddot{y} + (k_2 + k_1)\dot{y} + (k_1k_2 - \alpha_2\beta\lambda_f^2)y = \beta\lambda_f f_n(t) \tag{4.5}$$

is obtained. The solution to this equation may be written as

$$y = \Phi_n(t) + A_n e^{-\kappa_1 t} + B_n e^{-\kappa_2 t} , \tag{4.6}$$

where

$$\kappa_1 = \frac{1}{2}\left[k_2 + k_1 + \sqrt{(k_2 - k_1)^2 + 4\alpha_2\beta\lambda_f^2}\right] , \tag{4.7a}$$

$$\kappa_2 = \frac{1}{2}\left[k_2 + k_1 - \sqrt{(k_2 - k_1)^2 + 4\alpha_2\beta\lambda_f^2}\right] , \tag{4.7b}$$

$$\Phi_1(t) = \frac{(\alpha_0 + \alpha_1)\beta\lambda_f\lambda_L}{k_1k_2 - \alpha_2\beta\lambda_f^2} - \frac{\alpha_1\beta\lambda_f\lambda_L e^{-\alpha_3 t}}{(k_1 - \alpha_3)(k_2 - \alpha_3) - \alpha_2\beta\lambda_f^2} , \tag{4.8a}$$

$$\Phi_2(t) = \frac{\beta\lambda_f\alpha_3\ell_0 e^{-\alpha_3 t}}{(k_1 - \alpha_3)(k_2 - \alpha_3) - \alpha_2\beta\lambda_f^2} . \tag{4.8b}$$

Combining these results with Eq. 4.2 yields

$$x = \Theta_n(t) + \frac{k_2 - \kappa_1}{\beta\lambda_f} A_n e^{-\kappa_1 t} + \frac{k_2 - \kappa_2}{\beta\lambda_f} B_n e^{-\kappa_2 t} , \tag{4.9}$$

where

$$\Theta_1(t) = \frac{(\alpha_0 + \alpha_1)k_2\lambda_L}{k_1k_2 - \alpha_2\beta\lambda_f^2} - \frac{\alpha_1\lambda_L(k_2 - \alpha_3)e^{-\alpha_3 t}}{(k_1 - \alpha_3)(k_2 - \alpha_3) - \alpha_2\beta\lambda_f^2} , \tag{4.10a}$$

$$\Theta_2(t) = \frac{\alpha_3\ell_0(k_2 - \alpha_3)e^{-\alpha_3 t}}{(k_1 - \alpha_3)(k_2 - \alpha_3) - \alpha_2\beta\lambda_f^2} . \tag{4.10b}$$

The most general boundary conditions are

$$\text{As} \quad t \longrightarrow 0, \quad x \longrightarrow x_0 \quad \text{and} \quad y \longrightarrow y_0 . \tag{4.11}$$

Inserting these conditions into Eqs. 4.6 and 4.9, the integration constants become

$$A_n = \frac{k_2 - \kappa_2}{\kappa_1 - \kappa_2}[y_0 - \Phi_n(0)] - \frac{\beta\lambda_f}{\kappa_1 - \kappa_2}[x_0 - \Theta_n(0)] \tag{4.12a}$$

and

$$B_n = -\frac{k_2 - \kappa_1}{\kappa_1 - \kappa_2}[y_0 - \Phi_n(0)] + \frac{\beta\lambda_f}{\kappa_1 - \kappa_2}[x_0 - \Theta_n(0)] . \tag{4.12b}$$

In this report three special cases will be considered:

Case I. *Reactor operation starting with "clean" condition.* – The poisoning is given by Eq. 4.9, using the function 4.10*a*. The integration constants are found from Eqs. 4.12*a* and *b*, using $x_0 = y_0 = 0$ and the quantities $\Phi_1(0)$ and $\Theta_1(0)$.

Case II. *Reactor operation at zero nuclear power, after a period of high-power operation.* – The poisoning is given by Eq. 4.9, using the function 4.10*b*. The initial conditions are found from solutions to the problem of case I. In this instance $\lambda_L = 0$, and the quantity $\mathcal{I}_0$ is found from the equation

$$\alpha_3 \mathcal{I}_0 = \alpha_1 \lambda_L' (1 - e^{-\alpha_3 t'}) , \tag{4.13}$$

where λ_L' is the value of λ_L for the preceding period of high-power operation and t' is the time of operation.

Case III. *Sparging of reactor after a period of complete shutdown, during which no xenon is removed.* – The poisoning is given by Eq. 4.9, using the function $\Theta_2(t)$. In this case $\lambda_L = 0$, $y_0 = 0$, and $\mathcal{I}_0$ is found from

$$\alpha_3 \mathcal{I}_0 = \alpha_1 \lambda_L' (1 - e^{-\alpha_3 t'}) e^{-\alpha_3 t''} , \tag{4.14}$$

where t'' is the time between the shutdown and the time $t = 0$. The quantity x_0 is calculated from

$$x_0 = x_0^0 e^{-\alpha_4 t''} + \frac{\alpha_1 \lambda_L'}{\alpha_4 - \alpha_3} (1 - e^{-\alpha_3 t'}) (e^{-\alpha_3 t''} - e^{-\alpha_4 t''}) , \tag{4.15}$$

where x_0^0 is the poisoning at reactor shutdown, found from the solution to the problem of case I.

In dealing with cases II and III above, it is of interest to know whether or not the quantities x and y reach their extreme values (maxima) at the same time. When x reaches its maximum value, from Eqs. 4.1 and 4.2, then

$$k_1 \dot{y}^* = \beta \lambda_f f_2^* - (k_1 k_2 - \alpha_2 \beta \lambda_f^2) y^* , \tag{4.16}$$

where the asterisks indicate the special time value. It can readily be shown that the coefficients of f_2^* and of y^* are both always positive quantities. Thus $\dot{y}^*$ can vanish only if

$$y^* = \frac{\beta \lambda_f}{k_1 k_2 - \alpha_2 \beta \lambda_f^2} f_2^* . \tag{4.17}$$

Comparison of this equation with Eq. 4.6 shows that Eq. 4.17 cannot be satisfied in general, so that the extreme behavior of x and y cannot be examined by studying the differential equations alone.

5. STEADY-STATE OPERATION OF A REACTOR

For very long times of high-power operation, the poisoning reaches a steady-state value. From Eqs. 4.12 and 4.7, the steady-state values of x and y are[6]

$$x_\infty = \frac{(\alpha_0 + \alpha_1)k_2\lambda_L}{k_1k_2 - \alpha_2\beta\lambda_f^2} \tag{5.1}$$

and

$$y_\infty = \frac{(\alpha_0 + \alpha_1)\lambda_L\beta\lambda_f}{k_1k_2 - \alpha_2\beta\lambda_f^2} = \frac{\beta\lambda_f}{k_2}\, x_\infty \ . \tag{5.2}$$

These relations can be used in estimating the steady-state poisoning of a reactor under various conditions. The most convenient way to make these estimates is first to calculate

$$\lambda_p^\infty = \frac{\lambda_f(\alpha_4 + \lambda_g)}{\alpha_4 + \lambda_g + \alpha_2\beta\lambda_f} \ . \tag{5.3}$$

This result is obtained by substituting Eqs. 5.1 and 5.2 into Eq. 3.8. If the mean lives

$$\tau_p^\infty = \frac{1}{\lambda_p^\infty} \tag{5.4a}$$

and

$$\tau_f = \frac{1}{\lambda_f} \tag{5.4b}$$

are now introduced, then

$$\tau_p^\infty = \tau_f + \frac{\alpha_2\beta}{\alpha_4 + \lambda_g} \ . \tag{5.5a}$$

Since $\alpha_4 \ll \lambda_g$, this expression may be rewritten as

$$\tau_p^\infty = \tau_f + \frac{RTS\ V_L}{v_G} \ . \tag{5.5b}$$

Then x_∞ is computed through the relationship

$$x_\infty = \frac{(\alpha_0 + \alpha_1)\lambda_L}{\alpha_4 + \lambda_L + \lambda_p^\infty} \ . \tag{5.6}$$

The data in Table 2 have been used to estimate the steady-state poisoning, x_∞, in the ART for various assumed values of the phase-transfer mean life. The results are presented in Fig. 2.

It is of interest to examine briefly the expected behavior of ART-type reactors of higher power. Although the poisoning of an unsparged reactor of this type is essentially independent

---

[6] By an argument similar to that at the end of Sec. 4, it may be shown that x and y do not reach steady-state values simultaneously. Equations 5.1 and 5.2 apply only after both quantities reach steady state.

TABLE 2. DATA FOR NUMERICAL CALCULATION

Numerical Data

$\alpha_0 = 0.254\%$	$R = 82.0567$ cc-atm/mole/°K
$\alpha_1 = 4.74\%$	$T = 1033$°K (1400°F)
$\alpha_2 = 0.0509$	$S = 6 \times 10^{-7}$ moles/cc-atm[a]
$\alpha_3 = 2.87 \times 10^{-5}$ sec^{-1}	$\sigma_{Xe} = 1.7 \times 10^{6}$ barns[b]
$\alpha_4 = 2.09 \times 10^{-5}$ sec^{-1}	

Reactor Data

	ARE[c]	ART[d]
V_L	5.35 ft^3	5.64 ft^3
V_G	1 ft^3	0.31 ft^3
v_G	0.25 cc/sec	1000 STP liters/day
ϕ	8×10^{11} neutrons/cm^2/sec	1×10^{14} neutrons/cm^2/sec
β	5.35	18.2
λ_L	1.36×10^{-6} sec^{-1}	1.7×10^{-4} sec^{-1}

[a] R. F. Newton, personal communication.
[b] W. K. Ergen and H. W. Bertini, *ANP Quar. Prog. Rep. March 10, 1955*, ORNL-1864, p 16.
[c] J. L. Meem, personal communication and *ARE Nuclear Log Book*, ORNL Classified Notebook 4210.
[d] H. T. Furgerson and J. L. Meem, personal communication.

of power, very large increases in poisoning are possible with increased power when efficient sparging is employed. Only the most optimistic case will be considered, with $\tau_f = 0$. Equation 5.6 may then be written as

$$x_\infty = \frac{(\alpha_0 + \alpha_1)\lambda_L}{\lambda_L + (v_G/RTS\,V_L)} \quad . \tag{5.7}$$

If there are no major differences in design of such a reactor and in particular if the fuel volume and dilution factor are about the same as in the ART, the poisoning may be estimated on the basis of ART data, by simply adjusting λ_L in proportion to the power change. The results are presented in Fig. 3.[7]

[7] A scale for the amounts of helium required may be visualized by noting that an ordinary cylinder of helium contains 220 scf of gas (6230 liters). It may also be remarked that if τ_f is about 5 min, requiring 5000 STP liters of helium per day to maintain about 0.5% poisoning in a 300-Mw reactor, and if the aircraft flies at a speed of 1000 mph (about Mach 1.3 at sea level), the plane will get some 18 miles per gallon of helium.

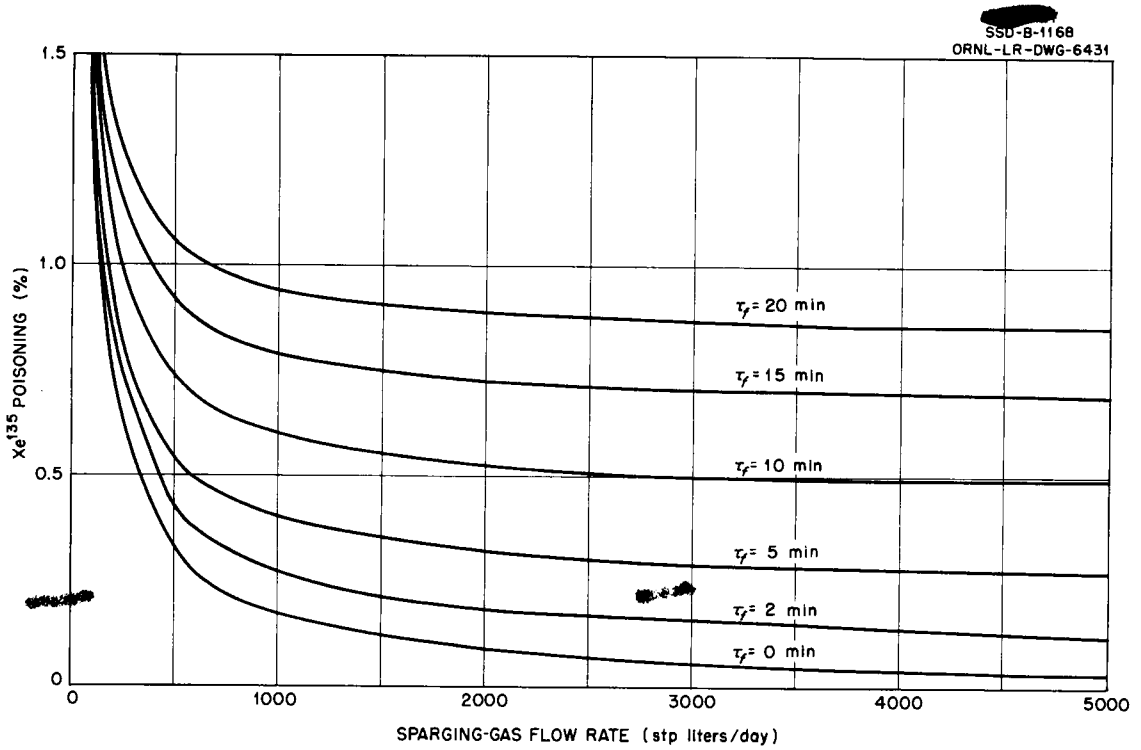

Fig. 2. Steady-State Xe^{135} Poisoning in the ART as a Function of Sparging-Gas Flow Rate for Various Assumed Values of the Phase-Transfer Mean Life τ_f.

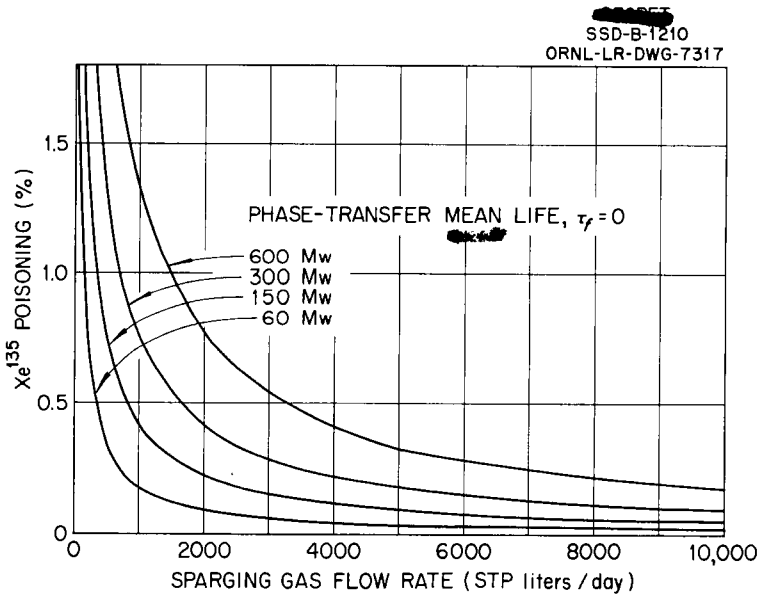

Fig. 3. Steady-State Xe^{135} Poisoning in ART-Type Reactors as a Function of Sparging-Gas Flow Rate for Various Assumed Reactor Powers.

Apparently, other things being equal, the sparging-gas flow rate must increase linearly with power, to maintain constant poisoning. It should be noted that while a decreased fuel volume increases the term $[v_G/(RTS\ V_L)]$ in Eq. 5.7, this is roughly compensated by a corresponding increase in λ_L, which is proportional to the volume-averaged flux.

6. KINETICS OF Xe^{135} POISONING IN THE ARE

An extensive series of calculations has been performed on the Oracle,[8] to aid in studying the approach to steady state of the Xe^{135} poisoning in the ARE. Typical results are presented in Figs. 4 through 7.

Figure 4 illustrates the dependence of the Xe^{135} poisoning kinetics on the value of λ_f. Note that curves for all values of $\lambda_f \geq 6 \times 10^{-3}$ sec^{-1} fall together on the scale chosen in the

[8] Coding and supervision of the calculations were done by C. L. Gerberich, ORNL Mathematics Panel. Results were obtained by using Eqs. 4.1, 4.2, and 3.8, together with numerical data from Table 2, except as noted in the text.

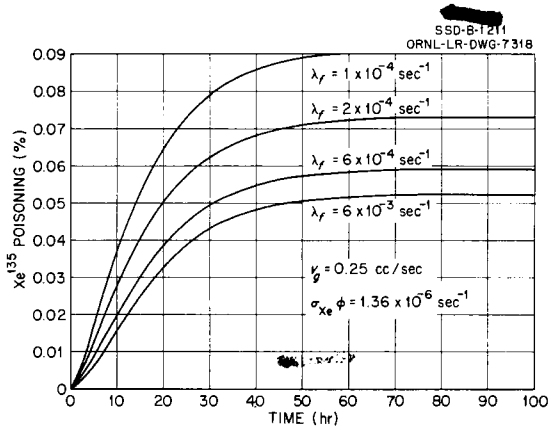

Fig. 4. Effect of λ_f on Xe^{135} Purging in the ARE.

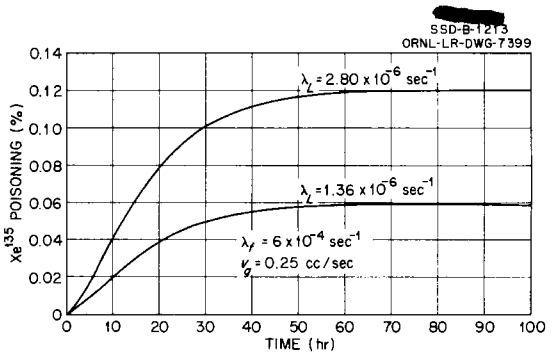

Fig. 6. Effect of λ_L on Xe^{135} Poisoning in the ARE.

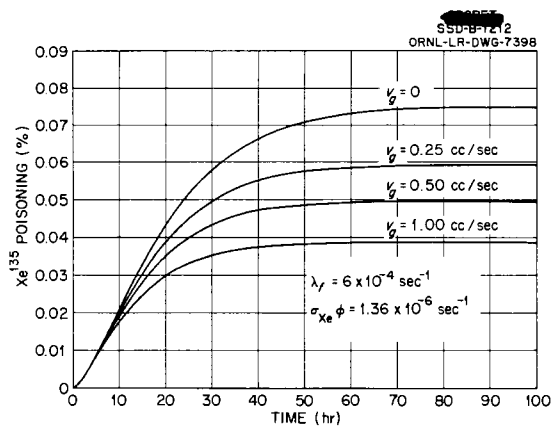

Fig. 5. Effect of Sparging-Gas Flow Rate on Xe^{135} Poisoning in the ARE.

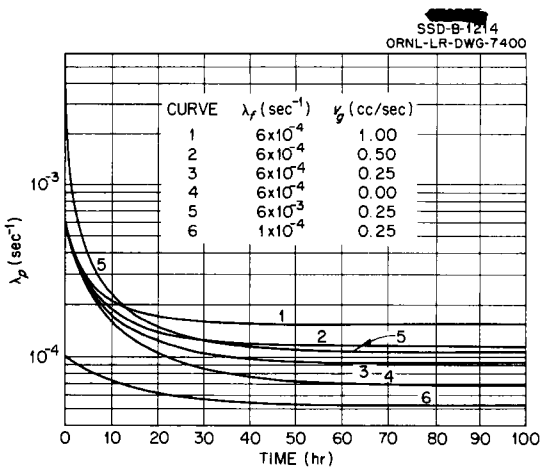

Fig. 7. Variation of the Apparent Purge Constant with Time in the ARE.

figure. This results from the small volumetric flow rate of off gas in the ARE. This flow rate is rate-determining, making an accurate estimate of λ_f from experimental data difficult.

Figure 5 illustrates the poisoning effects that occur as a result of variations in the sparging-gas flow rate, v_G, at a value $\lambda_f = 6 \times 10^{-4}$ sec^{-1}. A comparison of Figs. 3 and 4 shows that at early times (up to 10 hr or so) the rate of Xe^{135} removal is primarily governed by the rate of phase transfer, while for longer times the gas flow rate becomes controlling. Thus, under ARE conditions, fission-gas removal may be termed "off-gas controlled."

Figure 6 illustrates the effects of λ_L on poisoning kinetics. As might be anticipated, the results are roughly proportional to λ_L.

Figure 7 presents results on the time dependence of λ_p, which is called here the "apparent rate constant" for transfer of Xe^{135} from fuel to off gas. The large decrease in λ_p with time is clearly evident. Note also that $d\lambda_p/dt$ is everywhere negative.

Theory and experiment may be compared as follows.[9] By employing the abbreviations

$$f(t) = \alpha_0\lambda_L + \alpha_1\lambda_L(1 - e^{-\alpha_3 t}) \tag{6.1a}$$

and

$$g(t) = \alpha_4 + \lambda_L + \lambda_p(t) , \tag{6.1b}$$

the differential equation 2.16 may be written as

$$\dot{x}(t) = f(t) - g(t)x(t) . \tag{6.2}$$

Expanding each of the functions in Eq. 6.2 about the origin,

$$x(t) = \dot{x}_0 t + \frac{\ddot{x}_0 t^2}{2} + \frac{\dddot{x}_0 t^3}{6} + \cdots , \tag{6.3a}$$

$$f(t) = f_0 + \dot{f}_0 t + \frac{\ddot{f}_0 t^2}{2} + \cdots , \tag{6.3b}$$

$$g(t) = g_0 + \dot{g}_0 t + \frac{\ddot{g}_0 t^2}{2} + \cdots , \tag{6.3c}$$

where the subscript zero represents values at the origin ($t = 0$). If Eqs. 6.3*a*, *b*, and *c* are introduced into Eq. 6.2 and if the coefficient of each power of t is equated to zero, then

$$\dot{x}_0 = f_0 = \alpha_0\lambda_L , \tag{6.4a}$$

$$\ddot{x}_0 = \dot{f}_0 - f_0 g_0 = (\alpha_1\alpha_3 - \alpha_0 g_0)\lambda_L , \tag{6.4b}$$

---

[9] This approach was suggested by D. K. Holmes, ORNL Solid State Division.

$$\dddot{x}_0 = \dddot{f}_0 - \dot{f}_0 g_0 - f_0(g_0^2 + 2\dot{g}_0) = -[\alpha_1\alpha_3^2 + \alpha_1\alpha_3 g_0 + \alpha_0(g_0^2 + 2\dot{g}_0)]\lambda_L \qquad (6.4c)$$

$$\vdots$$

Now, in principle, a set of experimental data may be fitted to a power series (Eq. 6.3*a*), and the various coefficients of the series (Eq. 6.3*c*) can be determined from Eqs. 6.4*a*, *b*, and *c*. Note that from Eq. 3.8

$$\lambda_p(0) = \lambda_f \ ,$$

so that the value of the coefficient g_0 (i.e., the behavior of the poisoning near the origin) is of primary concern.

The experimental data on poisoning in the ARE[10] are given in Table 3, along with calculated contributions due to Sm^{149} and to burnup of U^{235}. The neutron capture cross section of Sm^{149} was taken as 53,000 barns,[11] and the burnup effect was calculated from[11]

$$\left(\frac{\Delta k}{k}\right)_{\text{burnup}} = \frac{0.232\Delta M}{M} \ ,$$

where k is the infinite multiplication constant and M is the mass of U^{235} in the reactor. Other data were taken from Table 2. Since the Sm^{149} and burnup contributions are well within the experimental error in the total poisoning, the experimental results are taken to apply to Xe^{135} poisoning alone.

The results from the ARE cannot be treated by the method described above for two major reasons:

1. The ARE data are based on the assumption that the origin of the (x,t) coordinates was at the start of the experiment. Since about 7 hr of high-power operation preceded the "xenon experiment,"[10] both I^{135} and Xe^{135} were present in the core at the time "zero" in Table 3.

[10] *ARE Nuclear Log Book*, ORNL Classified Notebook 4210.

[11] S. Glasstone and M. C. Edlund, *Elements of Nuclear Reactor Theory*, p 338, Van Nostrand, New York, 1952.

TABLE 3. EXPERIMENTAL DATA ON ARE POISONING

Time (hr)	Total Poisoning (%)	Calculated Poisoning (%)		
		Burnup	Sm^{149}	Xe^{135}
0	0	0	0	0
1.3	0.003 ± 0.001	0.0001	0.0000	0.004
12.7	0.006 ± 0.002	0.0006	0.0003	0.110
13.7	0.009 ± 0.002	0.0006	0.0003	0.119
16.0	0.012 ± 0.002	0.0007	0.0004	0.144
20.2	0.015 ± 0.003	0.0009	0.0006	0.182

2. Application of the method outlined above requires knowledge of λ_L. This quantity governs the scale of the x-coordinate. For the present calculations, a value of 1.36×10^{-6} sec^{-1} was assumed, based on 1.7×10^6 barns for the Xe^{135} cross section and 8×10^{11} neutrons/cm^2/sec for the ARE thermal flux.

It has recently been shown that the Xe^{135} cross section in the ARE is nearer 1.4×10^6 barns.[12] The flux value employed was based on the values 575 barns for the U^{235} fission cross section; 173 Mev per fission absorbed in the reactor; fuel density 3.24 g/cc; composition 13.59 wt % uranium, 93.4% enriched; and 2 Mw reactor power. The resulting value for the flux is not more precise than ±20%. It does not appear possible to expect agreement better than about a factor of 2 between theory and experiment.

On this basis, results from the ARE have merely been compared with calculated curves similar to those of Fig. 4. It is concluded that λ_f must be larger than about 5×10^{-4} sec^{-1} and is probably around 1×10^{-3} sec^{-1}.

7. KINETICS OF Xe^{135} POISONING IN THE ART

In this section the results of Oracle computations of the time dependence of the Xe^{135} poisoning in the ART are presented and discussed. The data employed are those of Table 2, except as noted. Typical results are shown in Figs. 8 through 12.

[12] W. K. Ergen and H. W. Bertini, *ANP Quar. Prog. Rep. March 10, 1955*, ORNL-1864, p 16.

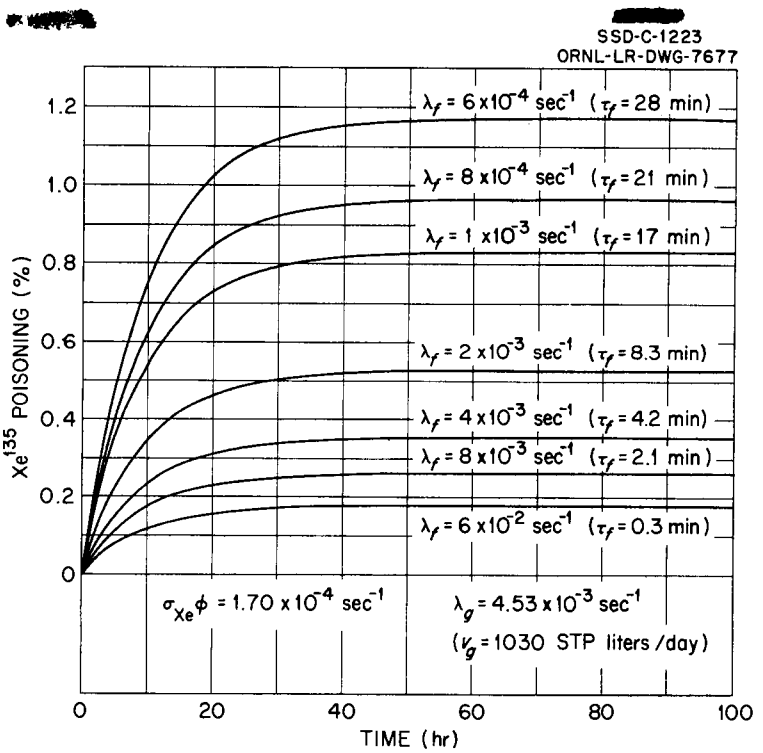

Fig. 8. Effect of λ_f on Xe^{135} Poisoning Kinetics in the ART.

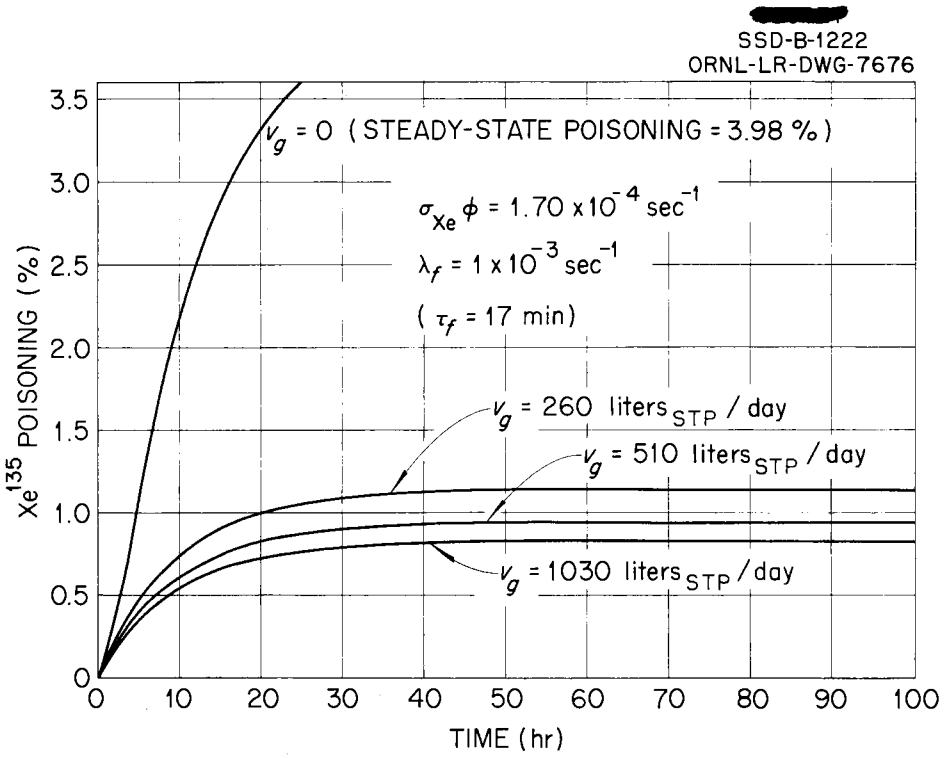

Fig. 9. Effect of Sparging-Gas Flow Rate on ART Poisoning Kinetics.

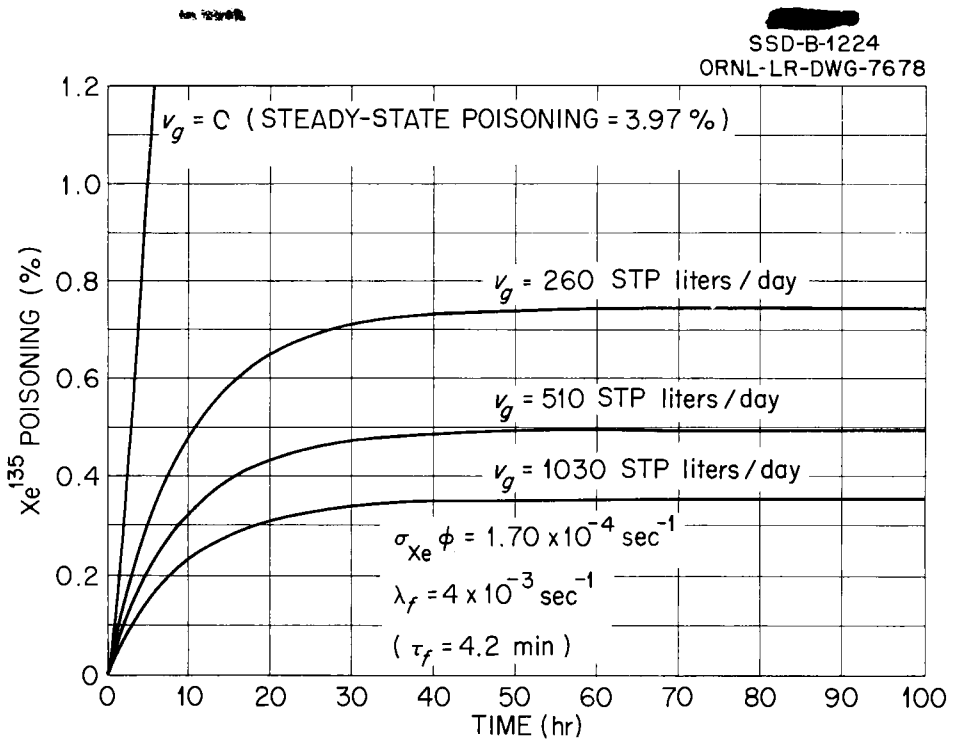

Fig. 10. Effect of Sparging-Gas Flow Rate on ART Poisoning Kinetics.

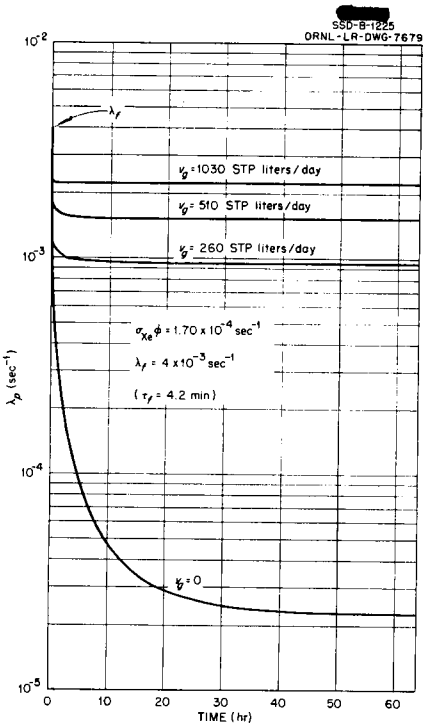

Fig. 11. Time Dependence of the Apparent Rate Constant λ_p in the ART.

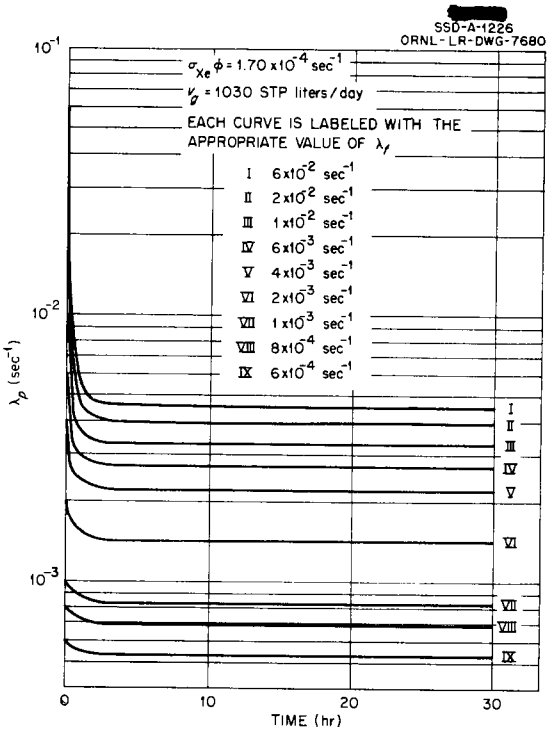

Fig. 12. Time Dependence of the Apparent Rate Constant λ_p in the ART.

Figure 8 illustrates the dependence of poisoning kinetics on the value of λ_f, for a value of $\lambda_g = 4.53 \times 10^{-3}$ sec^{-1} (ν_g = 1030 STP liters/day).[13] The effects of sparging-gas flow rate are presented in Figs. 9 and 10 for two different values of λ_f. Because of the much higher sparging-gas flow rates, the ART will not be as insensitive to the rate of phase transfer as was the ARE. Examination of Figs. 9 and 10 shows that the reactor will be more sensitive to off-gas flow rate if λ_f is comparatively small than it will if λ_f is comparatively large. Poisoning kinetics in the ART can be termed neither "off-gas controlled" nor "phase-transfer controlled," both processes being appreciably rate determining.

The time behavior of the apparent rate constant, λ_p, is somewhat different from that in the ARE, because of the much greater sparging-gas flow rate in the ART. Examination of Figs. 11 and 12 shows that at high gas flow rates λ_p reaches its steady-state value very rapidly – only about 3 hr being required, compared with about 40 hr in the ARE. Physically, this means that the gas phase in the ART reaches a steady state with the fuel phase very rapidly.

Because of the rapid approach to steady state of λ_p, it is possible to use the approximate method of Sec. 9 for rapid calculations of ART poisoning kinetics.

---

[13] In converting the values of λ_g to the values of ν_g quoted, it has been assumed that the gas pressure in the ART swirl chamber was about 2 psig. Then ν_g (STP liters/day) = $2.27 \times 10^5 \lambda_g$ (sec^{-1}).

8. KINETICS OF Xe^{135} POISONING DURING SHUTDOWNS[14]

In this section a brief analysis will be made of the expected behavior of the Xe^{135} poisoning of the ART during shutdowns. For this purpose the equations derived in Sec. 4 for cases II and III will be employed.

First to be considered is a shutdown of nuclear power during which fuel flow and sparging are continued. The reactor is assumed to have been at steady state prior to shutdown. The data given in Table 2 for the ART are chosen, with τ_f taken as 5 min. The result is not shown since values for all the terms other than the one for I^{135} decay are always negligible. Under the assumed conditions, the poisoning will not rise by as much as 1 or 2% of the steady-state value. It is thus concluded that decreases in reactor power will cause no troublesome transient increase in the Xe^{135} poisoning in reactors of the ART type.

A more serious problem is concerned with the growth of xenon during a total shutdown. The behavior of the ART is examined in this regard by assuming that after the reactor reaches steady-state operation it is shut down totally and the xenon is allowed to grow in until it reaches its maximum concentration. At this point, sparging is started and continued, at zero nuclear power. It is necessary to determine how rapidly the poisoning can be reduced to the high-power steady-state level. The behavior in this respect governs in large part the amount of "xenon override" which must be built into the reactor. The data used are from Table 2, with $\tau_f = 5$ min. The maximum poisoning was calculated from Eq. 4.15.

After the reactor is shut down, the Xe^{135} poisoning rises to a maximum of about 12%. If no sparging were used, it would then decrease slowly, reaching the full-power steady-state value in about 70 hr. During almost all this time, operation of the reactor would be impossible with the control rod presently proposed for the ART. However, if sparging is started at the time of maximum Xe^{135} concentration (11.2 hr after shutdown), rapid reduction in poisoning occurs. Figure 13 shows that Xe^{135} is reduced to the full-power steady-state value in about 36 min. Since this time is less than that necessary to start up the ART after a total shutdown,[15] there seems to be no reason to provide large amounts of "xenon override" in the control rod. This statement remains true even if τ_f is significantly larger than the value used here.

9. NOMOGRAMS FOR XENON-POISONING CALCULATIONS

Two simple nomograms have been constructed to speed rough calculations of Xe^{135} poisoning. *Nomogram 1* (Fig. 14) describes the steady-state poisoning

$$x_\infty = \frac{(\alpha_0 + \alpha_1)\lambda_L}{\lambda_L + \alpha_4 + \lambda_p} , \qquad (9.1)$$

---

[14] Although it is somewhat illogical to use the term "poisoning" in discussing conditions during a reactor shutdown, it is convenient to do so. Difficulties are thus avoided in comparing shutdown conditions with those during nuclear power operation.

[15] W. B. Cottrell, personal communication.

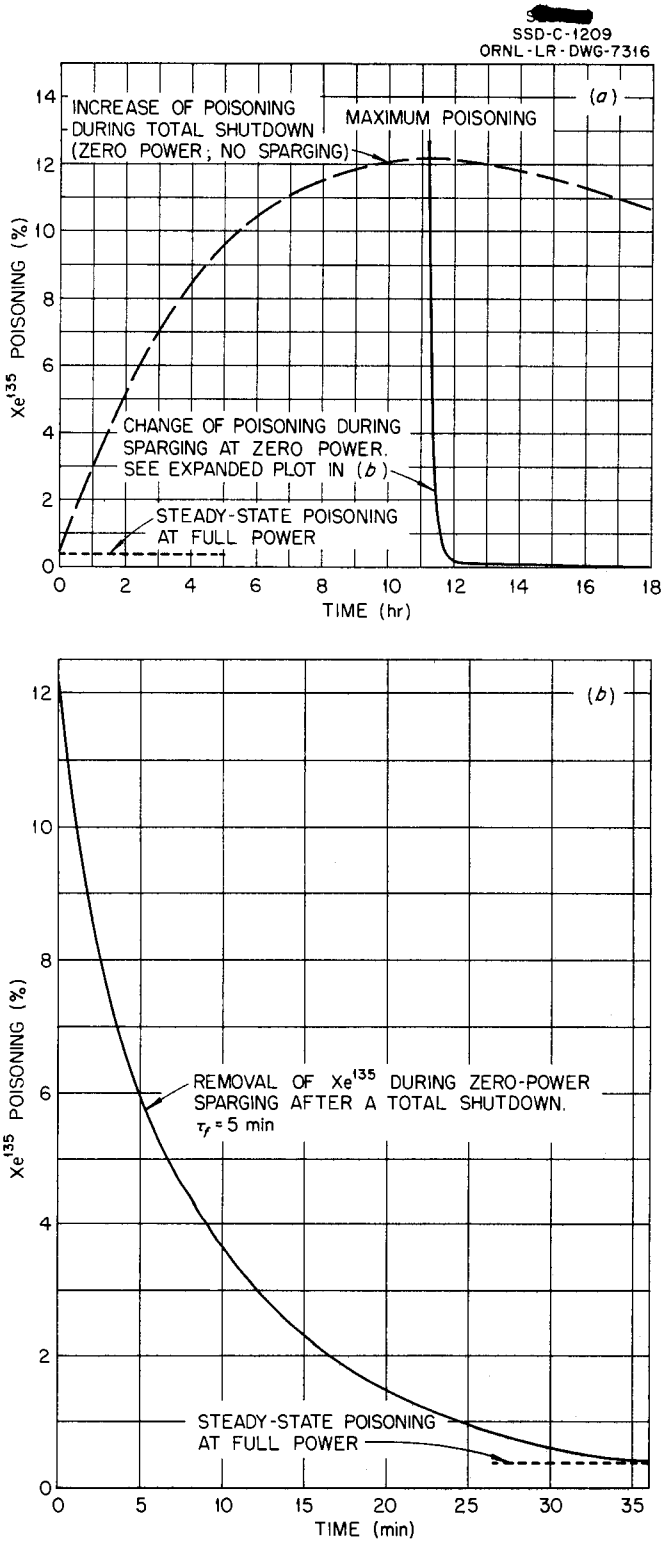

Fig. 13. Behavior of Xe^{135} Poisoning in the ART During Shutdowns.

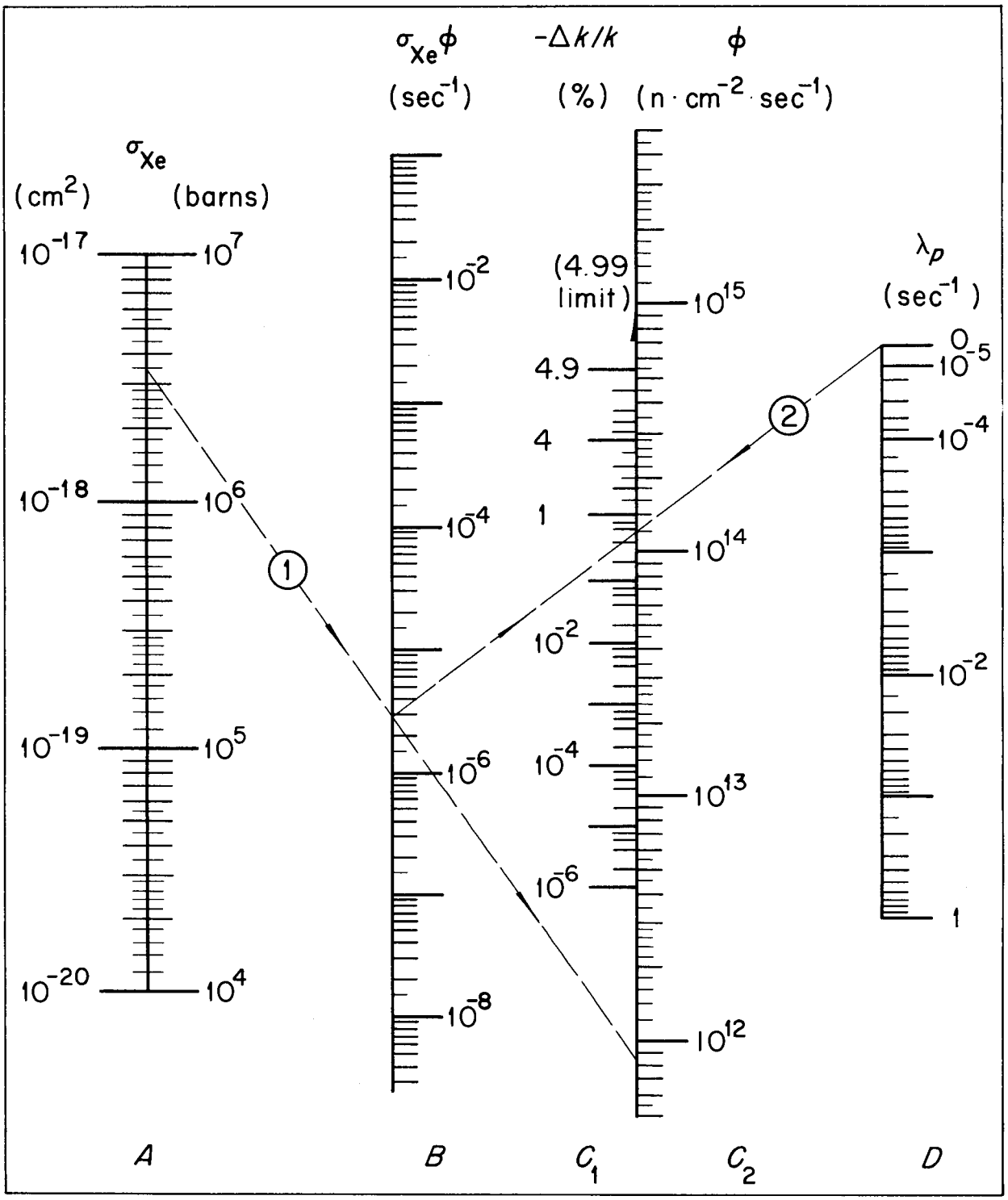

Fig. 14. Nomogram 1: Steady-State Xe^{135} Poisoning.

where all symbols are defined in Table 1 and values are given in Table 2. To derive the nomogram, let

$$U = \log \left[\frac{\alpha_0 + \alpha_1}{x_\infty} - 1 \right] , \tag{9.2a}$$

$$V = \log (\lambda_p + \alpha_4) , \tag{9.2b}$$

$$W = \log \lambda_L . \tag{9.2c}$$

Then, introducing Eqs. 9.2 into Eq. 9.1, the equation for bars B, C_1, D of the nomogram is

$$U = V - W . \tag{9.3}$$

Furthermore, by letting

$$Z = \log \sigma_{Xe} , \tag{9.4a}$$

$$S = \log \phi , \tag{9.4b}$$

the equation of bars A, B, C_2 may be written

$$W = Z + S . \tag{9.5}$$

The five bars are laid off with linear scales in the variables S, Z, U, V, and W. The distances between bars is

$$\overline{AB} = \overline{BC} = \overline{CD} . \tag{9.6}$$

To use nomogram 1, lay a straightedge from the value of σ_{Xe} on bar A to the value of ϕ on bar C_2, locating their product (λ_L) on bar B. Lay the straightedge from this point on bar B to the value of λ_p on bar D, locating x_∞ on bar C_1. The procedure is illustrated by an example shown on the nomogram by faint dashed lines.

Nomogram 2 (Fig. 15) describes the approach of the poisoning to its steady-state value. The equation employed is

$$\xi = \frac{x}{x_\infty} = 1 - e^{-at} - \frac{ab}{a - \alpha_3} (e^{-\alpha_3 t} - e^{-at}) , \tag{9.7}$$

where

$$a = \alpha_4 + \lambda_L + \lambda_p ,$$

$$b = \frac{\alpha_1}{\alpha_0 + \alpha_1} = 0.949 .$$

To derive the nomogram, let

$$U = e^{-at} , \tag{9.8a}$$

$$V = e^{-\alpha_3 t} , \tag{9.8b}$$

$$W = \frac{ab}{a - \alpha_3} . \tag{9.8c}$$

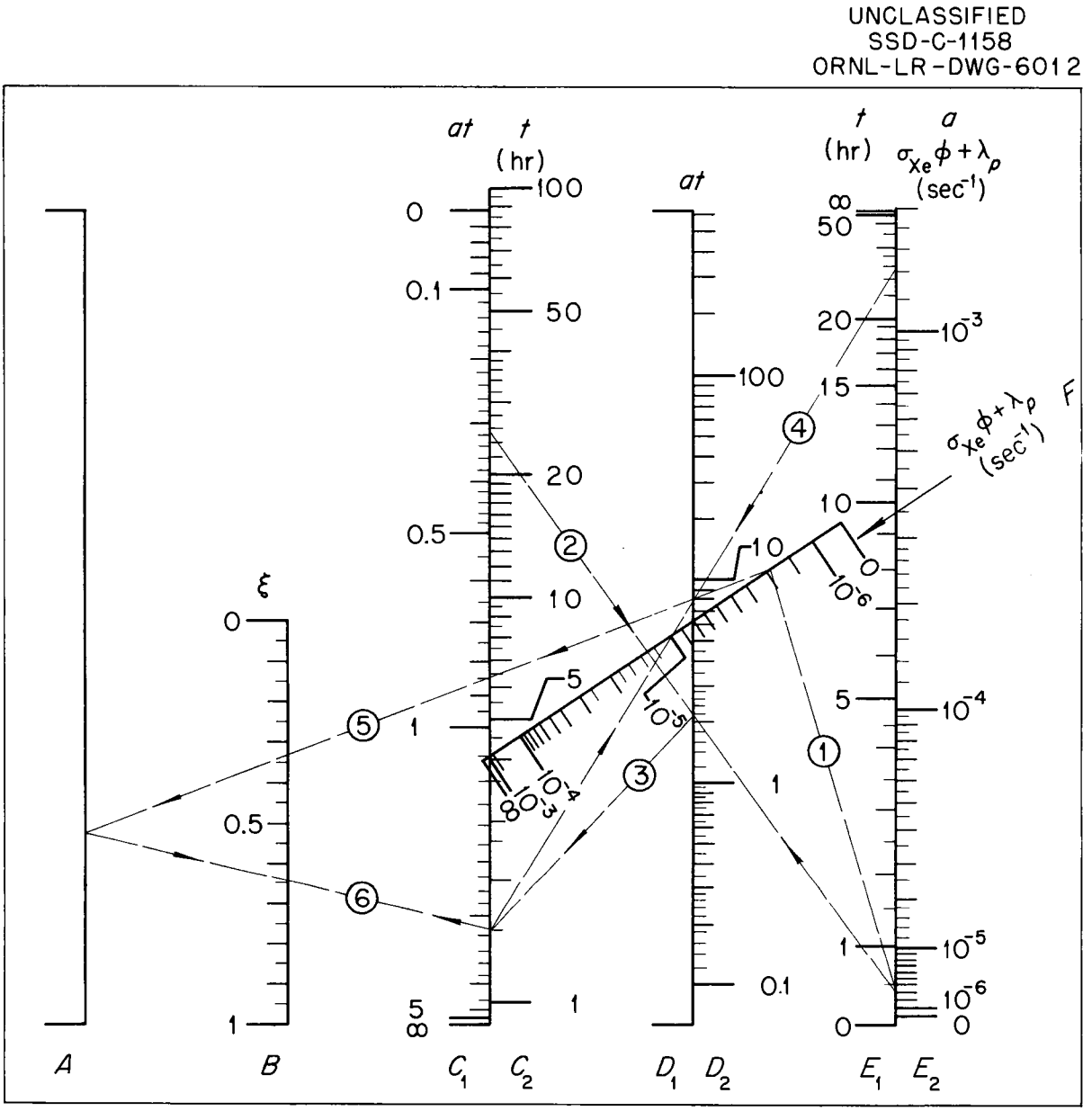

Fig. 15. Nomogram 2: Time Dependence of Xe^{135} Poisoning.

[redacted]

Then Eq. 9.7 becomes

$$\xi = 1 - U - W(U - V) \ . \tag{9.9}$$

Further, let

$$Z = W(U - V) = 1 - U - \xi \ . \tag{9.10}$$

Bars C_1, E_1, D_1 are linear scales in the variables U, V, and $(U - V)$, respectively, the subtraction being performed on this subnomogram. Since the numerical value of $(U - V)$ is not required, no scale is inscribed on bar D_1. Bars A, F, D_1 constitute a nomogram for the operation

$$Z \cdot \frac{1}{W} = (U - V) \ . \tag{9.11}$$

Bar A is a linear scale in Z. Bar F is a scale in $(1/W)$, constructed to obey Eq. 9.11, with the Z and $(U - V)$ scales both linear. Bars A, C_1, and B constitute a nomogram for the operation

$$\xi = 1 - U - Z \ . \tag{9.12}$$

Bar B is linear in the variable ξ. The bars C_2, D_2, E_2 are used as a subsidiary nomogram to perform the operation

$$\log (at) = \log a + \log t \ . \tag{9.13}$$

These bars are linear in the variables log t, log at, and log a, respectively. The distances between the five vertical bars are

$$\overline{AB} = \overline{BC} = \overline{CD} = \overline{DE} \ . \tag{9.14}$$

Bar F is laid off between the origins of bar A $(Z = 0)$ and bar D_1 $[(U - V) = 0]$.

To use nomogram 2, proceed as follows: From bar B of nomogram 1, read the value of $\lambda_L = \sigma_{X_e}\phi$ and add to it the value λ_p. Enter this result on *both* bars E_2 and F. Lay a straightedge from the desired time on bar C_2 to the value on bar E_2, locating the value (at) on bar D_2. Transfer this value to bar C_1. Now lay the straightedge from bar C_1 to the desired time on bar E_1, locating a point on bar D_1. Lay the straightedge from this point on bar D_1 to the value marked on bar F, locating a point on bar A. Finally, lay the straightedge from bar A to the point marked on bar C_1, locating the desired value ξ on bar B. The procedure is illustrated by an example shown on the nomogram by faint dashed lines.

The accuracy of these nomograms is limited by the precision of the input data, the process of drawing, and the means of reproduction. It is believed that the versions given in this report are accurate to around ±5%.

[redacted]